Effect of Metal Cations on the Conformation of Myosin Subfragment-1-ADP-Phosphate Analog Complexes: A Near-UV Circular Dichroism Study†

Y. Michael Peyser,‡ Katalin Ajtai,§ Moshe M. Werber,|| Thomas P. Burghardt,§ and Andras Muhlrad*,‡

Department of Biochemistry and Molecular Biology, Mayo Foundation, Rochester, Minnesota 55905, Department of Oral Biology, Hebrew University-Hadassah School of Dental Medicine, Jerusalem, Israel 91120, and Biotechnology General, Kiryat Weizmann, Rehovot 76236, Israel

Received February 3, 1997⊗

ABSTRACT: The interaction of myosin with actin, coupled with hydrolysis of ATP, is the molecular basis of muscle contraction. The head segment of myosin, called S1, contains the distinct binding sites for ATP and actin and is responsible for the ATPase activity. The myosin-catalyzed ATP hydrolysis consists of several intermediate steps and each step is accompanied by conformational changes in the S1 segment. The rate-limiting step of the ATP hydrolysis is the dissociation of the S1·ADP·P_i complex which is accelerated by actin. The substitution of P_i with phosphate analogs (PA), such as vanadate, beryllium fluoride (BeF_x) or aluminum fluoride (AlF_4^-), yields stable complexes which mimic the intermediates of the ATP hydrolysis. In this work, tertiary structure changes in S1 in the vicinity of aromatic residues was studied by comparing near-UV circular dichroism (CD) spectra from S1−nucleotide−phosphate analog complexes in the presence of Mg^{2+} and other cations. A significant difference between the MgATP and MgADP spectra indicated notable tertiary structural changes accompanying the M**ADP·P_i → M*ADP transition. The spectra of the S1·MgADP·BeF_x and S1·MgADP·AlF_4^- complexes resemble to those obtained upon addition of MgATPγS and MgATP to S1, and correspond to the M*·ATP and M**·ADP·P_i intermediates, respectively. We have found recently that the presence of divalent metal cations (Me^{2+}) is essential for the formation of stable S1·MeADP·PA complexes. Moreover, the nature of the metal cations strongly influences the stability of these complexes [Peyser, Y. M., et al. (1996) *Biochemistry 35*, 4409−4416]. In the present work we studied the effect of Mg^{2+}, Mn^{2+}, Ca^{2+}, Ni^{2+}, Co^{2+}, and Fe^{2+} on the near-UV CD spectrum of the ATP, ADP, ADP·BeF_x, and ADP·AlF_4^- containing S1 complexes. The CD spectra obtained with ADP, ATP ADP·BeF_x and ADP·AlF_4^- were essentially identical in the presence of Co^{2+} and rather similar in the case of Ca^{2+}, while they were partially different in other cases. An interesting correlation was found between actin activation and ATP versus ADP difference spectra in the presence of various metal ions. The distribution of the fractional concentration of the intermediates of ATP hydrolysis was estimated in the presence of each cation from the CD spectra with phosphate analogs. In the presence of Mg^{2+} the predominant intermediate is the M**·ADP·P_i state, which is in accordance with the kinetic studies. On the other hand with non-native cations the predominant intermediate is the M*·ADP state and the release of ADP is the rate limiting step in the myosin-catalyzed ATP hydrolysis. According to the results, the near-UV CD spectrum originating from aromatic residues in S1 not only can distinguish identifiable states in the ATP hydrolysis cycle but can also pinpoint to changes in the tertiary structure caused by complex formation with nucleotide or nucleotide analog and various divalent metal cations. These findings, that are correlative with actin activation, and thus with the power stroke, suggest new strategies for perturbing S1 structure in the continuous efforts directed toward the elucidation of the mechanism of muscle contraction.

The force production by the myosin motor in muscle is based on the interaction of myosin heads with actin, which is coupled to ATP hydrolysis. According to Bagshaw and Trentham (1973), the myosin-catalyzed ATP hydrolysis takes place in several stages as shown in eq 1

$$\mathrm{M} + \mathrm{ATP} \overset{1}{\leftrightarrow} \mathrm{M^*{\cdot}ATP} \overset{2}{\leftrightarrow} \mathrm{M^{**}{\cdot}ADP{\cdot}P_i} \overset{3}{\leftrightarrow} \mathrm{M^*{\cdot}ADP} + \mathrm{P_i} \overset{4}{\leftrightarrow} \mathrm{M} + \mathrm{ADP} + \mathrm{P_i} \quad (1)$$

where M represents myosin, or its active proteolytic fragments including myosin subfragment 1 (S1),[1] and one or two asterisks symbolize specific conformational changes taking

† This research was supported by NIH Grant R01AR39288, AHA Grant 93006610, and the Mayo Foundation (T.P.B. and K.A.).

* Corresponding author.
‡ Hebrew University.
§ Mayo Foundation.
|| Biotechnology General.

⊗ Abstract published in *Advance ACS Abstracts,* April 1, 1997.

[1] Abbreviations: S1, myosin subfragment 1; S1Dc, truncated *Dictyostelium* S1; Me^{2+}, metal divalent cation; PA, phosphate analog; V_i, vanadate; P_i, inorganic phosphate; PP_i, pyrophosphate; BeF_x, beryllium fluoride complex; AlF_4^-, aluminum fluoride complex; ATPγS, adenosine-5′-*O*-3-thiotriphosphate; CD, circular dichroism.

S0006-2960(97)00255-9 CCC: $14.00

place in the protein during the various stages of ATP hydrolysis. These conformational changes were indicated by several observations, such as increase in tryptophan fluorescence emission (Werber et al., 1972) and UV absorption (Morita & Yagi, 1966), altered reactions rate of reactive thiols (Reisler et al., 1977) and lysines (Muhlrad & Fabian, 1970), as well as changes in the product pattern of limited trypsinolysis (Muhlrad & Hozumi, 1982; Applegate & Reisler, 1984) and intramolecular cross-linking (Blotnick & Muhlrad, 1995). Since the dissociation of P_i in stage 3 is the rate-limiting step of the ATP hydrolysis the M**·ADP·P_i complex is the predominant intermediate of the myosin catalyzed ATP hydrolysis. Actin, the other main structural protein of muscle, highly accelerates the release of P_i from the M**·ADP·P_i complex, and the dissociation of P_i is closely associated with the generation of force (power stroke) in the cross-bridge cycle during muscle contraction. Because of the central role of the ATP hydrolysis in muscle contraction it is essential to characterize the structure of each intermediate in the process. However, this is difficult because of the short life time of the intermediates. Analog compounds, which form not (or form only slowly) transforming complexes with myosin and resemble the various intermediates of ATP hydrolysis, may contribute to solve the problem of the stability in structural studies. Such an analog is ATPγS whose myosin complex resembles the prehydrolyzed M*·ATP state and the structural analogs of P_i — vanadate (V_i), beryllium fluoride (BeF_x), and aluminum fluoride (AlF_4^-) complexes — which can substitute P_i in the M**·ADP·P_i complex and resemble various intermediate states prior to the dissociation of P_i (Goodno, 1979; Phan & Reisler, 1992; Werber et al., 1992). The complexes of the recombinant truncated *Dictyostelium* S1 with BeF_x and AlF_4^-, S1dC·MgADP·BeF_x and S1dC·MgADP·AlF_4^-, were recently crystallized and their atomic structure was resolved (Fisher et al., 1995). These studies have shown significant structural differences between the two complexes and indicated that S1dC·MgADP·BeF_x and S1dC·MgADP·AlF_4^- resemble the M*·ATP and M**·ADP·P_i intermediate states, respectively. In the light of the importance of conformation changes in S1 during the ATP hydrolysis it is of interest to record the near-UV CD spectra of the S1−nucleotide and S1−nucleotide−phosphate analog complexes since altered near-UV CD spectra can indicate changes, which take place in the tertiary structure of the protein in the vicinity of aromatic residues (Strickland, 1974). We found that the CD spectrum of S1·MgADP·BeF_x closely resembles that of S1·MgATPγS modeling the prehydrolyzed M*·ATP state, while the spectrum of S1·MgADP·AlF_4^- loosely resembles to that of M**·ADP·P_i.

Divalent metal cations play also an essential role in the myosin-catalyzed ATP hydrolysis. Under physiological conditions the nucleotide is chelated with Mg^{2+} which highly contributes to the stability of the M**·ADP·P_i complex (Bagshaw & Trentham, 1974). *In vitro*, other divalent cations including Ca^{2+}, Mn^{2+}, Co^{2+}, Ba^{2+}, Sr^{2+}, Fe^{2+}, Ni^{2+}, and Zn^{2+} are able to substitute Mg^{2+} in the myosin-catalyzed ATP hydrolysis (Yount & Koshland, 1963; Seidel, 1969; Peyser et al., 1996). Myosin also catalyzes the hydrolysis of ATP in the absence of divalent cations, provided certain monovalent cations are present. However, under these circumstances the product release (steps 3 and 4) is much faster, while the ATP cleavage (step 2) is slower than in the presence of divalent cations (Lymn & Taylor, 1970). Moreover, nucleotide cannot be trapped into the active site of S1 by BeF_x and V_i phosphate analogs in the absence of divalent cations (Peyser et al., 1996). All these emphasize the substantial role of divalent cations in the formation of S1−nucleotide complexes. It has been shown that Mg^{2+} could be replaced in the trapped S1·MgADP·V_i complex by Ca^{2+}, Ni^{2+}, or Mn^{2+} (Grammer et al., 1988); however, no comprehensive study was carried out to reveal the contribution of divalent cations to the formation and stability of the S1−nucleotide complexes. Recently we studied the effect of various divalent cations, including Mg^{2+}, Mn^{2+}, Ca^{2+}, Ni^{2+}, Co^{2+}, and Fe^{2+} on the ATPase activity of S1 in the presence and absence of actin; and on the formation and decomposition of the BeF_x and/or V_i containing stable S1−ADP complexes (Peyser et al., 1996). It was observed in these studies that all metal cations employed could replace Mg^{2+} in the actin-activated S1 ATPase; however, their effect on both the V_{max} and the K_M of the reaction was different from that of Mg^{2+}. The various cations influenced differently the stability of the trapped S1−nucleotide complexes, as indicated by their effects on their formation and rate of decomposition. The results raised the possibility that the divalent metal cations affect the conformation of the S1−nucleotide complexes, and this was studied in the present work by measuring the near-UV CD spectra of the complexes. The CD spectra recorded showed that the metals indeed have a substantial effect on the conformation of S1 in the presence of nucleotides. A preliminary report of this work has been presented (Ajtai et al., 1996).

MATERIALS AND METHODS

Chemicals. ATP, ADP, phenylmethanesulfonyl fluoride, dithioerythritol, chymotrypsin, $BeCl_2$ (dissolved in 1% HCl), HEPES, Tris-HCl, and the chloride salts of the divalent cations were purchased from Sigma Chemical Co. ATPγS was purchased from Boehringer Mannheim. All other chemicals were of reagent grade. *Note: Beryllium is very toxic and should be handled carefully*. NaF and $FeCl_2$ stock solutions were daily prepared freshly. To the $FeCl_2$ stock solution dithioerythritol was added in stoichiometric concentration in order to prevent the oxidation of Fe(II).

Preparation of Proteins. Myosin was prepared from back and leg muscles of rabbit by the methods of Tonomura et al. (1966). S1 was obtained by digestion of myosin filaments with α-chymotrypsin as described by Weeds and Taylor (1975). Protein concentrations were obtained by absorbance, using A (1%) at 280 nm of 5.5 and 7.5 for myosin and S1, respectively. Molecular masses were assumed to be 500 and 115 kDa for myosin and S1, respectively.

ATPase Assay. K^+(EDTA)-activated ATPase activity (nanomoles of phosphate per milligram of S1 per minute) was calculated from the inorganic phosphate produced, measured according to Fiske and Subbarow (1925). The reaction was performed at 25 °C on 1-mL aliquots taken at various time intervals. Incubation time were chosen so that no more than 15% of the ATP was hydrolyzed. The reaction mixture contained 1 μM S1, 2 mM ATP, 6 mM EDTA, 600 mM KCl, and 50 mM Tris-HCl buffer, pH 8.0, and incubated at 25 °C for 2 min.

Circular Dichroism. Near-UV CD spectra were recorded in a 10 mm path length cuvette at 20 °C on a Jobin et Yvon

CD 6 spectropolarimeter (in Jerusalem, Israel) and on a JASCO J 720 spectropolarimeter (in Rochester, MN, USA). For each spectrum at least four scans were averaged. To 17 μM S1 in 30 mM HEPES buffer, pH 7.0, were added the chloride salts of the divalent metal cations in the following concentrations: Mg^{2+}, 1 mM; Co^{2+}, 0.1 mM; Mn^{2+}, 0.2 mM; Ca^{2+}, 1 mM; Ni^{2+}, 0.5 mM; Fe^{2+}, 0.1 mM. This was followed by addition of 0.2 mM ADP or ATPγS. After that 5 mM NaF and then 0.2 mM $BeCl_2$ or 0.8 mM $AlCl_3$ was added, and the mixture was incubated at 20 °C for 20 min for the development of the trap. In samples containing MeATP an ATP-regenerating system (5 μM pyruvate kinase and 5 mM phosphoenolpyruvate) was added to keep the ATP concentration constant. Since the formation of the trap is accompanied by the inhibition of the K^+(EDTA)-activated ATPase activity of S1, this was checked with each cation. The lowest concentration of metal cation sufficient to cause at least 90% inhibition of ATPase activity was used in the CD measurements as indicated above. Under each condition the CD spectrum was recorded also in the absence of S1 and was subtracted to obtain curves for the S1 containing complexes. The CD data for each wavelength were expressed as molar ellipticity, [Θ] (deg cm^2 dmol^{-1}):

$$[\Theta] = 100\Theta_\lambda/Cl$$

where Θ_λ is the measured ellipticity in degrees at a given wavelength, l is the optical path length in cm, and C is the molar concentration of S1.

Calculation of ATPase Intermediate State Concentrations. We compared the CD spectrum from MeATP-S1 to that from phosphate analog trapped S1 to estimate the steady-state fractional concentrations of the ATPase intermediates. Using eq 1 we modeled the CD molar ellipticity spectrum from MeATP-S1 with

$$\text{MeATP-S1} = a_1\text{MeADPBeF}_x\text{−S1} + a_2\text{MeADPAlF}_4\text{−S1} + a_3\text{MeADP−S1} \quad (2)$$

where the a_i's are unknown fractional concentrations of the intermediates in MeATP−S1 when the CD molar ellipticity spectrum from the analogs MeADPBeF$_x$−S1, MeADPAlF$_4$−S1, and MeADP−S1 mimic spectra from M*·ATP, M**·ADP·P$_i$, and M*·ADP, respectively. We constrain the model in eq 2 by requiring each spectrum to contribute appropriately ($a_i \geq 0$) while conserving molar ellipticity ($\sum_i a_i = 1$). A constrained linear least squares protocol determines the best choices for ai over all observed wavelengths (Strang, 1986).

RESULTS

Effect of Nucleotides and Phosphate Analogs on the Near-UV CD Spectrum of S1. The near-UV CD spectra of S1 in the presence of Mg, MgPP$_i$, and Mg−nucleotides, including phosphate analogs, are shown in Figure 1 (in two parts). The insets show the difference spectra of the various complexes versus MgS1. Significant changes were observed in the 255−292 nm region of the CD spectrum of S1 with all three nucleotides and two phosphate analogs, whereas MgPP$_i$, which has been shown to bind to the active site of myosin (Smith & Rayment, 1995), has a very small positive effect at 277 and 284 nm. According to Strickland (1974) and 255−270, 270−285, and 275−305 nm regions of the CD spectrum are mainly dominated by phenylalanine, tyrosine, and tryptophan residues, respectively. In the 275−285 nm region both tyrosine and tryptophan residues contribute to the spectrum. In the 255−265 nm region ATP (S1 is predominantly in M**·ADP·P$_i$ state) and ATPγS have a positive effect on the spectrum of S1, the influence of ATP being especially strong, while ATPγS, whose complex with S1 mimics the M*·ATP state, has a much weaker effect. The influence of ADP is practically negligible in this wavelength range. In the 265−292 nm region the nucleotides have negative effects, except for M**·MgADP·P$_i$ state where the negative effect appeared only in the 273−293 nm region. Here the effect of added nucleotides decrease the order ADP > ATPγS > ATP. Interestingly in the 292−305 nm region, which is dominated by ^1L_b transitions of tryptophans (Strickland, 1974), there is only a very weak, non-significant nucleotide effect.

The effect of "trap" formation in the presence of MgADP with either BeF$_x$ or AlF_4^- phosphate analogs (PA) on the near-UV CD spectrum of S1 is best understood by comparing the [Θ] values at various wavelengths of the difference spectra in two pairs: ATPγS versus ADP·BeF$_x$ and ATP (M**·MgADP·P$_i$) versus ADP·AlF_4^- (Table 1). In addition, the nucleotides versus MgS1 difference spectra presented in the insets of Figure 1. From the comparisons it can be deduced that the spectrum obtained in the presence of MgADP·BeF$_x$ is similar to that observed upon addition of ATPγS to S1 in the whole wavelength region recorded whereas the S1·MgADP·AlF_4^- spectrum shows similarity — at least in the 272−305 nm region — to the spectrum with MgATP, when S1 is predominantly in the M**·ADP·P$_i$ state.

Effect of Divalent Metal Cations on the Near-UV CD Spectra of S1−Nucleotide Complexes. The addition of Mg^{2+}, Mn^{2+}, Co^{2+}, Fe^{2+}, Ca^{2+}, and Ni^{2+} to S1 in the absence of nucleotides either did not influence the CD spectrum in the case of Mg^{2+}, Mn^{2+}, and Co^{2+}, or had a small, unspecific effect upon addition of Fe^{2+}, Ca^{2+}, and Ni^{2+} (not shown). Fe^{2+} and Ca^{2+} caused an increase in the whole spectrum monitored (255−305 nm), while addition of Ni^{2+} induced a decrease in the 255−273 and 295−305 nm regions.

The spectra of S1 with various metal cations measured in the absence of nucleotides and in the presence of ATP, ADP, ADP·BeF$_x$, and ADP·AlF_4^- are presented in Figures 2−6. In all cases the spectra recorded with and without nucleotides differed significantly. The presence of nucleotides caused a large decrease in the spectra in the region of the negative peak, 270−290 nm. However, the effects of ATP, ADP, ADP·BeF$_x$, and ADP·AlF_4^- were quite different in the presence of the various metal ions. Thus, in the presence of Mg^{2+} (Figure 1A) the ATP (S1**·MgADP·P$_i$) spectrum had a high positive amplitude, especially in the 257−267 nm region, in comparison to the other spectra and this was a special feature observed only in the presence of Mg^{2+} and not with other metals. In the presence of Mg^{2+} the ADP·BeF$_x$ spectrum ran between the ATP and the ADP spectra in the 255−280 nm region while the ADP·AlF_4^- spectrum was similar to the one obtained with ATP in the 272−305 nm region and ran below the ATP in the 255−272 nm region. On the other hand the ATP, ADP, ADP·BeF$_x$, and ADP·AlF$_4$ spectra were essentially identical with Co^{2+} and Mn^{2+}, except ADP·AlF$_4$ in the 255−272 nm region in the presence of Mn^{2+} (Figures 2 and 3). The effect of Fe^{2+} differed from

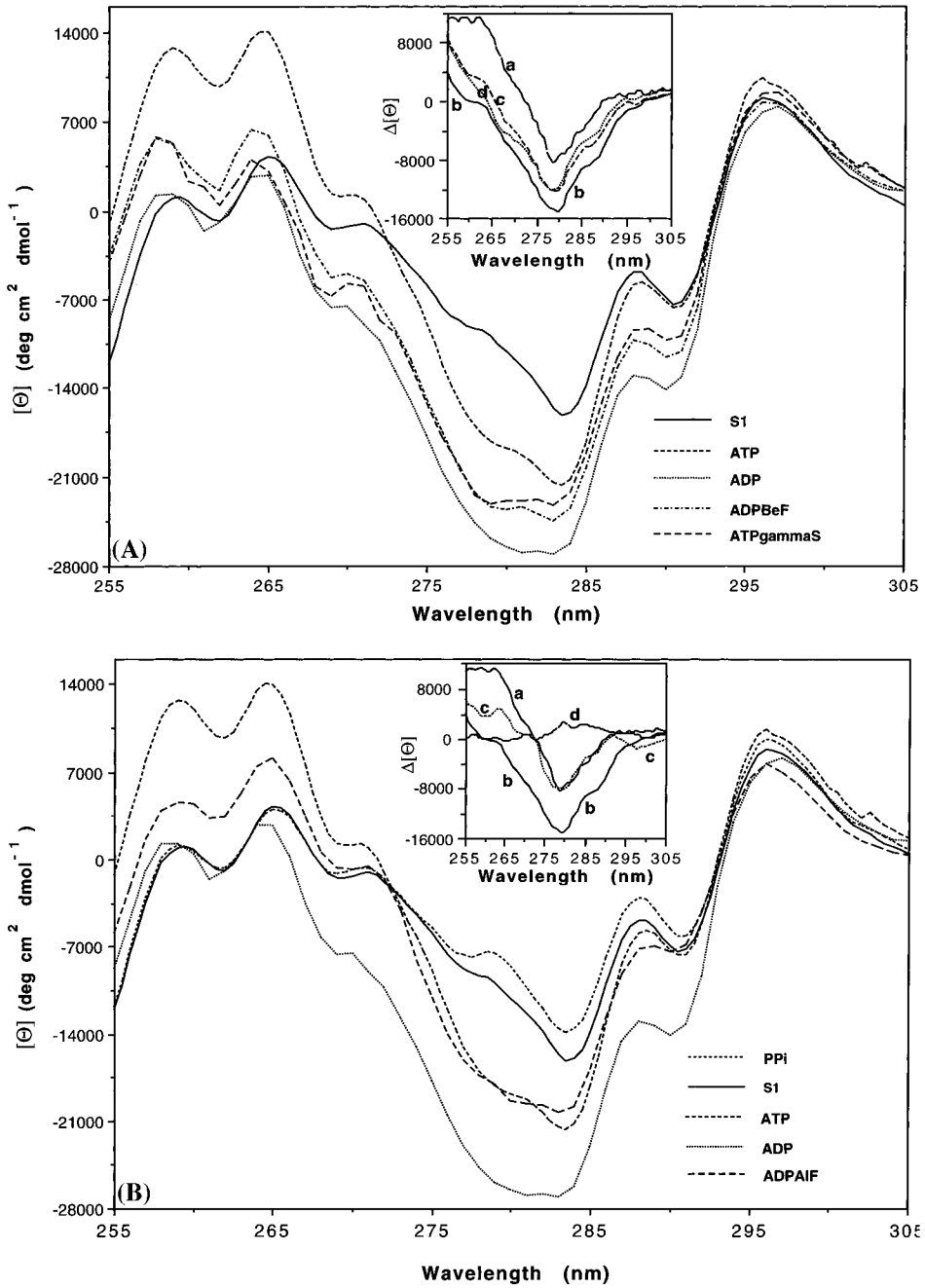

FIGURE 1: Effect of nucleotides, including phosphate analogs, and pyrophosphate on the near-UV CD spectrum of S1 in the presence of Mg^{2+}. For the details of the measurement see Methods. (A) S1, S1 + ATP, S1 + ADP, S1 + ATPγS, and S1 + ADP·BeF_x spectra. Inset: (a) S1·ATP − S1; (b) S1·ADP − S1; (c) S1·ADP·BeF_x − S1; (d) S1·ATPγS − S1 difference spectra. (B) S1, S1 + ATP, S1 + ADP, S1 + ADP·AlF_4^-, and S1 + PP_i spectra. Inset: (a) S1·ATP − S1; (b) S1·ADP − S1; (c) S1·ADP·AlF_4^- − S1; (d) S1·PP_i − S1 difference spectra.

Table 1: Molar Ellipticity Difference of S1·MgATPγS − S1·MgADP·BeF_x and S1·MgATP − S1·MgADP·AIF_4^- Spectra at Various Wavelengths

	wavelength (nm)			
spectrum	259	265	279	283
ATPγS − ADP·BeF_x ($\Delta[\Theta] \times 10^{-3}$)[a]	0.2	2.0	0.1	1.0
ATP − ADP·AlF_4^- ($\Delta[\Theta] \times 10^{-3}$)	7.2	4.9	0.0	0.5

[a] [Θ] is the molar ellipticity (deg cm^2 $dmol^{-1}$).

that of the other metals, since here in the presence of nucleotides the 279−280 nm trough was more negative than the 284 nm trough (Figure 4). In the presence of Fe^{2+} there were also some differences between the various nucleotide spectra, the ADP·BeF_x spectrum ran higher than the other three, and the ADP·AlF_4 spectrum ran much below all the others in the 255−272 nm region. The ATP and ADP spectra practically differed only in the 278−292 nm region. With Ca^{2+} the ADP·BeF_x spectrum was higher in the 255−272 nm region than the other three nucleotide spectra, which were essentially identical to this region. In the 272−295 nm region the nucleotide spectra decreased in the order ADP·AlF_4^- > ADP·BeF_x > ATP > ADP (Figure 5). In the case of Ni^{2+} the ADP·BeF_x and ADP·AlF_4^- spectra were not recorded since no trap formation was observed with these phosphate analogs in the presence of this metal cation. In this case, the ATP and ADP spectra were considerably

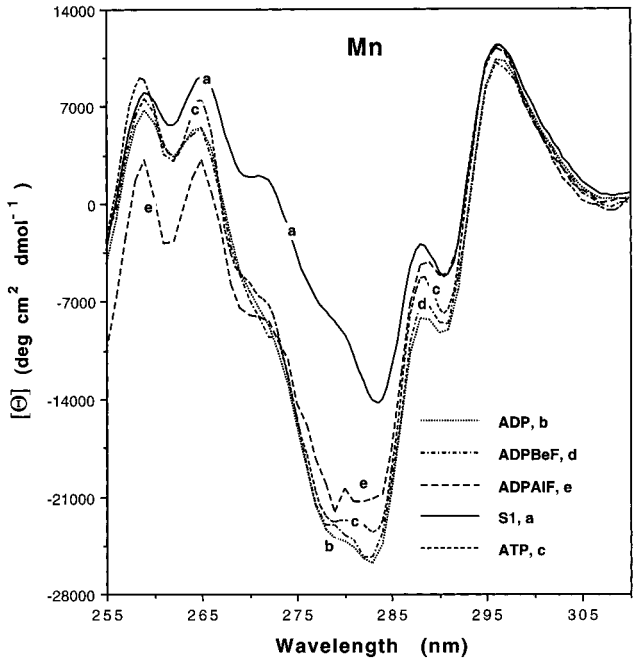

FIGURE 2: Effect of Mn^{2+} on the near-UV spectra of S1 in the presence of ADP, ATP, and ADP·BeF_x. (a) S1 + Mn; (b) S1 + MnADP; (c) S1 + MnATP; (d) S1 + MnADP·BeF_x; (e) S1 + MnADP·AlF_4^-. For the details of the measurements see Methods.

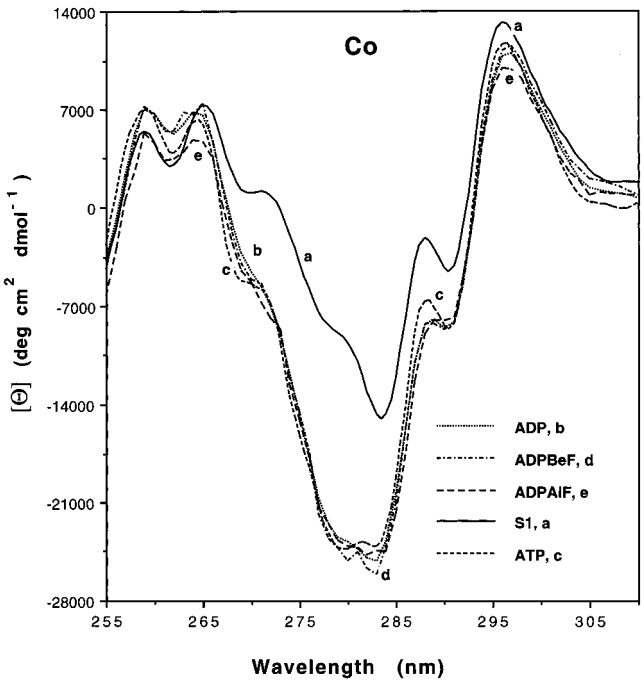

FIGURE 3: Effect of Co^{2+} on the near-UV spectra of S1 in the presence of ADP, ATP, and ADP·BeF_x. (a) S1 + Co; (b) S1 + CoADP; (c) S1 + CoATP; (d) S1 + CoADP·BeF_x; (e) S1 + CoADP·AlF_4^-. For the details of the measurements see Methods.

different from each other, and in the 255−283 nm region the ADP spectrum was blue shifted relative both to the ATP spectrum and to the spectrum obtained in the absence of nucleotide (Figure 6).

Another way to examine the differences between ATP and ADP spectra on the one hand and ADP·BeF_x and ADP spectra on the other hand is to express the $\Delta[\Theta]$ values at four wavelengths, 259, 265, 279, and 283 nm (Table 2). The major findings of this comparison are summarized below.

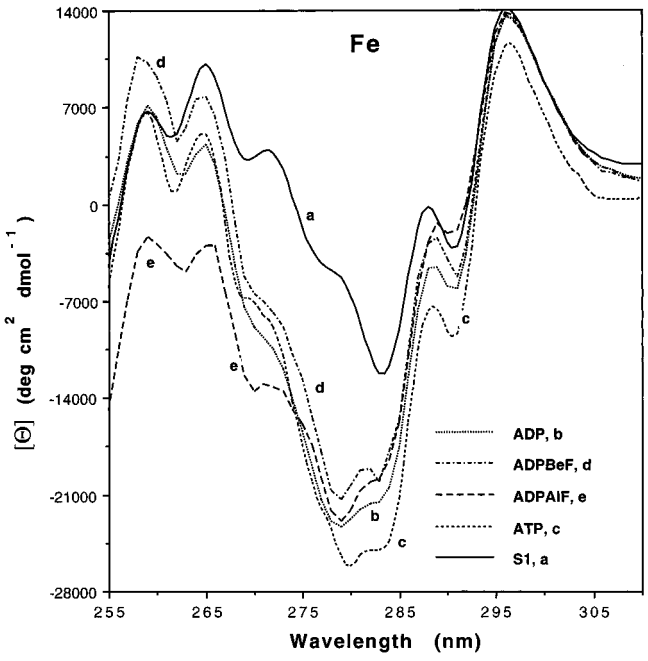

FIGURE 4: Effect of Fe^{2+} on the near-UV spectra of S1 in the presence of ADP, ATP, and ADP·BeF_x. (a) S1 + Fe; (b) S1 + FeADP; (c) S1 + FeATP; (d) S1 + FeADP·BeF_x; (e) S1 + FeADP·AlF_4^-. For the details of the measurements see Methods.

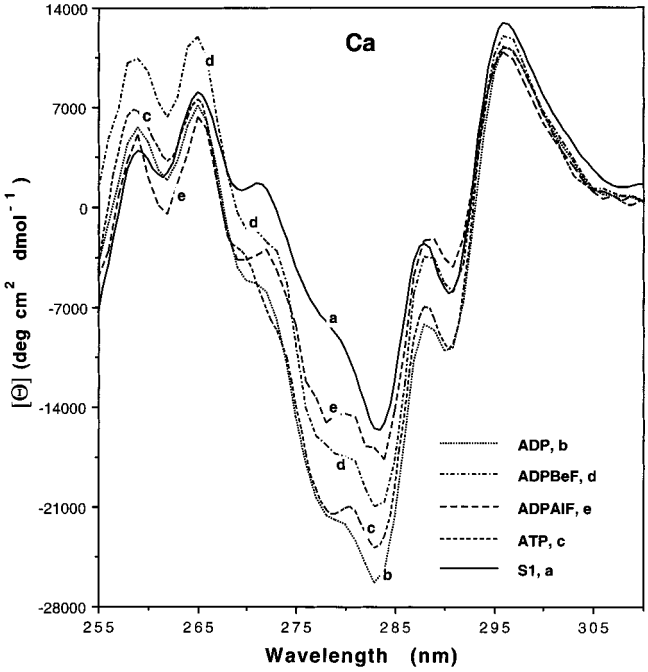

FIGURE 5: Effect of Ca^{2+} on the near-UV spectra of S1 in the presence of ADP, ATP, and ADP·BeF_x. (a) S1 + Ca; (b) S1 + CaADP; (c) S1 + CaATP; (d) S1 + CaADP·BeF_x; (e) S1 + CaADP·AlF_4^-. For the details of the measurements see Methods.

ATP versus ADP. Major positive changes only seen with Mg, both in the phenylalanine region, 259−265 nm, and in the tyrosine−tryptophan region, 279−283 nm, although in the latter region the change is smaller. Also Mn and Ca give positive changes in both regions, but these are 10−30% of the changes in Mg, and with Mn the changes are similar in both regions. With Co the changes are even smaller. With Fe quite large negative changes are seen, i.e., the ADP effect is larger than the ATP effect, mainly in the Tyr−Trp region. In the case of Ni, which is anomalous—probably because of the different geometry of

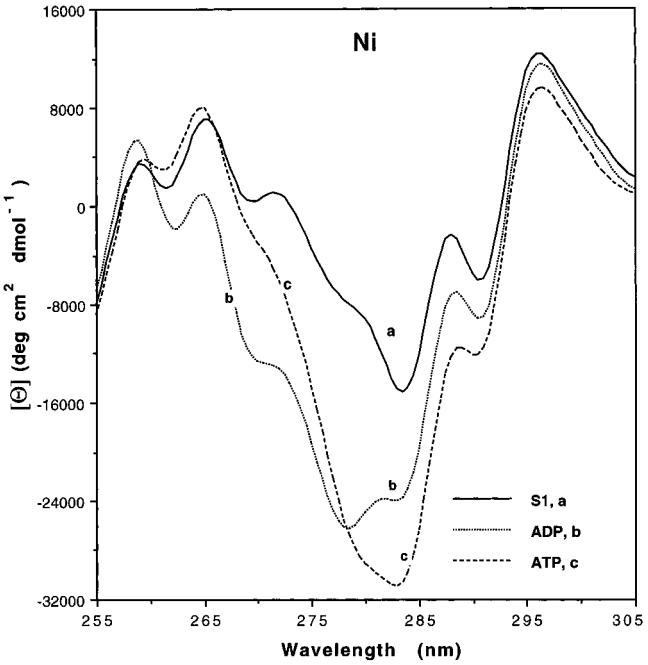

FIGURE 6: Effect of Ni^{2+} on the near-UV spectra of S1 in the presence of ADP, ATP, and ADP·BeF_x. (a) S1 + Ni; (b) S1 + NiADP; (c) S1 + NiATP. For the details of the measurements see Methods.

Table 2: Molar Ellipticity Difference of S1·MeATP − S1·MeADP, S1·MeADP·BeF_x − S1·MgADP, S1·MeATP − S1·MeADP·AlF_4^-, and S1·MgADP·AlF_4^- − S1·MeADP Spectra at Various Wavelengths

spectrum	wavelength (nm)	Δ[Θ] × 10^{-3} [a] Mg	Mn	Co	Fe	Ca	Ni
ATP − ADP	259	11.1	2.1	0	−0.4	1.2	−1.8
	265	11.2	2.0	−1.0	0.8	0.4	6.0
	279	6.9	1.3	−0.2	−2.3	0.5	−2.0
	283	6.4	2.4	1.1	−3.7	2.4	−6.8
ADP·BeF_x − ADP	259	4.0	0.8	0	2.9	4.8	
	265	3.3	0	0.4	3.7	3.1	
	279	2.8	1.1	−0.2	2.0	4.8	
	283	3.0	0.3	−1.0	1.3	5.2	
ATP − ADP·AlF_4^-	259	8.0	5.8	1.7	8.1	1.6	
	265	6.0	4.3	1.3	5.1	1.3	
	279	0.0	−0.7	−0.8	−0.9	−7.0	
	283	−1.1	−2.4	0.1	−5.5	−6.9	
ADP·AlF_4^- − ADP	259	3.8	−3.6	−1.7	−8.7	−0.5	
	265	5.5	−2.3	−2.0	−4.3	−0.5	
	279	7.9	1.9	−0.1	−1.2	7.3	
	283	6.9	4.7	1.1	2.0	9.2	

[a] [Θ] is molar ellipticity (deg cm^2 dmol^{-1}).

its complexes (see below)—both negative and positive effects are seen, the negative effects mainly in the Tyr−Trp region.

ADP·BeF_x versus ADP. The changes with Mg in both regions are less than half those of ATP. However, in this case Mg is not the only metal giving rise to this effect: Ca is at least as good as (better even in the Tyr−Trp region) and Fe is very similar to Mg. On the other hand, with Mn much smaller differences are observed, and with Co almost no effect is seen in the Phe region and a small negative effect in the Tyr−Trp region.

ATP versus ADP·AlF_4^-. (All differences compared to ATP minus ADP.)

Phe Region. In general, except for Mg, where the effect decreases slightly, with all cations the difference become significantly more positive: Fe and Mn values become similar to Mg, Co values become slightly positive from slightly negative, whereas almost no changes are seen with Ca. Overall, in this region the spectra obtained with MeADP·AlF_4 and MeATP states are quite different.

Tyr−Trp Region. Here the trends are reversed: positive effects become close to zero or even negative. Overall, it seems to show that for at least Mg, Co, and perhaps Mn, the ADP·AlF_4^- spectra are similar to the ATP spectra in this region while for Fe and Ca ADP·AlF_4^- and ATP spectra are quite different.

ADP·AlF_4^- versus ADP. (All differences compared to ADP·BeF_x minus ADP.)

Phe Region. The effect is generally more negative, in particular for Fe. Mg seems to be the exception and is slightly more positive. Overall, except Ca, it would seem to mean that the ADP·AlF_4^- spectra are further away from the MeADP than the MeADPBeF_x ones.

Tyr−Trp Region. The trend is reversed again, the effects are more positive, Mg, Mn and Ca leading the list and little effect with Co and Fe. Overall, it means that also in this region, with the exception of Co and Fe, the ADP·AlF_4^- spectra are more different from the ADP spectra than the ADP·BeF_x spectra.

Conclusion. For the ADP·AlF_4^- spectra the effects are very different in the two chromophoric regions.

Effect of Divalent Cations on the Distribution of ATPase Intermediates. We used eq 2 and the CD molar ellipticity spectra from S1·MeATP, S1·MeADPBeF_x, S1·MeADPAlF_4^-, and S1·MeADP to estimate the distribution of the M*·ATP, M**·ADP·P_i, and M*·ADP intermediates upon addition of MeATP to S1 for several divalent cations. Table 3 summarizes our results for the fractional concentrations of intermediates. We found that addition of MgATP to S1 at 20 °C results in fractional concentrations of 0.2, 0.8, and 0 for M*·ATP, M**·ADP·P_i, and M*·ADP, respectively, indicating that in this case P_i release is rate limiting. Similar results were obtained when S1·MgATPγS replaced S1·MgADP·BeF_x as the model for the M*·ATP intermediate. At 6 °C, the fractional concentrations indicated that the intermediate states are more uniformly populated. These data for the distribution of intermediates upon addition of MgATP resemble the results from Bagshaw and Trentham (1973). Table 3 shows that in the presence of Ca^{2+}, Co^{2+}, Mn^{2+}, and Fe^{2+} the predominant state during the ATP hydrolysis is M*·ADP, indicating that ADP release is rate limiting. In the presence of Ca^{2+} the M*·ATP intermediate is also significantly occupied unlike with the other non-native cations. We did not estimate the distribution of intermediates in the presence of Ni^{2+} because NiADP·AlF_4^- and NiADP·BeF_x did not stably trap S1.

We, therefore, propose that myosin ATPase without actin about equals the rate-limiting ADP release rate in the presence of the non-native cations, implying that the rates of ADP release are 0.32, 0.15, 0.20, and 0.19 s^{-1} for Ca^{2+}, Co^{2+}, Mn^{2+}, and Fe^{2+}, respectively, using the observed myosin ATPase rates in the presence of these cations [ATPases are taken from Peyser et al. (1996) and are listed in Table 3 for convenience]. We probably underestimate the CaADP release rate since the M*·ATP → M**·ADP·P_i transition contributes significantly to the ATPase of this cation.

Table 3: Effect of Divalent Cations on the Fractional Concentration of Intermediates in MeATP-S1 and the ATPases[a]

Me in MeATP−S1	M*·ATP	M**·ADP·P_i	M*·ADP	ATPase (s^{-1})[b]	V_{max} actin-activated ATPase (s^{-1})[c]
Mg	0.21	0.79	0.	0.04	14.7
Mg[d]	0.13	0.87	0.		
Mg[e]	0.19 ± 0.2	0.19 ± 0.2	0.62 ± 0.4		
Ca	0.17	0.06	0.77	0.32	7.1
Mn	0.	0.04	0.96	0.21	16.4
Co	0.	0.08	0.92	0.15	10.8
Fe	0.	0.	1.0	0.19	8.1

[a] CD spectra of S1 in the presence of MeATP were compared with S1·MeADP·BeF_x, S1·MeADP·AlF_4^-, and S1·MeADP spectra using eq 2 to estimate the fractional concentration of intermediates at 20 °C. Concentration errors are all ±0.1 standard error of the mean except when given explicitly. [b] S1 ATPase without actin at 25 °C. Values from Peyser et al. (1996). [c] V_{max} for actin-activated S1 ATPase at 25 °C. Values from Peyser et al. (1996). [d] MgATPγS replaced MgADP·BeF_x as the model for M*·ATP. [e] Experiment conducted at 6 °C.

DISCUSSION

The near-UV CD spectrum of proteins is dominated by the contributions of the aromatic amino acids Phe, Tyr, and Trp and of the disulfide moiety of cystine. Since S1 does not contain cystine residues, therefore, its whole near-UV CD spectrum, which consists of a number of peaks and troughs, is contributed by the aromatic residues. The aromatic rings of these residues acquire their near-UV CD bands through interactions with the peptide backbone or aromatic side chains in the protein. Features in the MgS1 spectrum from Figure 1 including the peaks at 259 and 265 and the troughs at 262 and 269 nm are likely generated by phenylalanine, while the peak at 271 nm is likely due to tyrosine residues. The peaks at 278 and 281 nm and the trough at 283 nm, which is the minimum of the spectrum, can be due to both tyrosine and tryptophan chromophores, while the 288 and 296 nm peaks and the 291 nm trough are generated only by tryptophans. The 283, 288, and 291 nm bands are probably due to ^1L_b, while the 296 nm band is due to ^1L_a transitions of the indole moiety of tryptophans (Strickland, 1974).

Addition of adenine nucleotides induces significant changes in the near-UV CD spectrum of S1. These changes may be generated by the interactions of the adenine moiety with the aromatic residues or by the nucleotide induced distortions in the S1 structure in the vicinity of the aromatic residues. Addition of $MgPP_i$, which is not a chromophore in the near-UV region and, like nucleotides, binds to the active site of myosin (Smith & Rayment, 1995) and induces conformational changes in S1 (Setton & Muhlrad, 1988), causes only very small changes in the near-UV CD spectrum of S1. Therefore, it is reasonable to assume that the nucleotide-induced difference spectra are generated by the interaction of the adenine moiety with the nearby aromatic residues. This does not exclude the possibility that nucleotide-induced conformational changes, which occur in a distance from the active site, could not contribute to the observed difference spectra. The largest spectral change upon addition of nucleotides was observed at 278 nm. This change can be generated by interaction of the adenine moiety with a tyrosine or a tryptophan residue. Since Tyr-134 and Trp-130 are proximal to the adenine moiety in the active site of myosin (Fisher et al., 1995), it is therefore probable that they contribute to the large negative peak observed at 278 nm in the nucleotide-induced difference spectra. Since pyrophosphate does not contain a purine or pyrimidine base, it does not induce any change in the CD spectrum in the 278 nm region. In addition to the large change in the 278 nm region a small but significant blue shift was observed upon addition of nucleotides in the 258−266 nm region, which is dominated by phenylalanine. This shift may reflect to nucleotide-induced increase in solvent accessibility of one or more Phe residues (Wood, 1994).

The near-UV CD spectra of S1 induced by addition of MgADP, MgATP, MgATPγS, MgADP·BeF_x, and MgADP·AlF_4^- (Figure 1) are not identical in spite of the fact that all of these nucleotides have the same absorption and CD spectra in the absence of S1. This indicates that the distance or the relative orientation (angle) of the neighboring aromatic residues to the adenine moiety of the nucleotide is different in the various S1−nucleotide complexes, or that these complexes induce different changes in the S1 structure — in the vicinity of aromatic residues — further away from the active site. In either case the findings point to conformational differences in the structure of various S1−nucleotide complexes. Since S1·MgATPγS, S1·MgATP, and S1·MgADP are generally believed to correspond to the successive M*·MgATP, M**·MgADP·P_i, and M*·ADP intermediates of the ATP hydrolysis, the findings are in accordance with the consensus view that conformational changes accompany the transitions of the myosin catalyzed ATP hydrolysis. The spectra of the stable (trapped) S1·MgADP·BeF_x and S1·MgADP·AlF_4^- complexes are similar to those obtained upon addition of MgATPγS and MgATP to S1, respectively. The S1·MgADP·AlF_4^- spectrum is less similar to the one obtained upon addition of MgATP to S1 (S1·MgADP·P_i spectrum) than that of S1·MgADP·BeF_x to the S1·MgATPγS spectrum. The results indicate that S1·MgADP·BeF_x is a structural model of M*·MgATP while S1·MgADP·AlF_4^- at least partially resembles the M**·ADP·P_i predominant transition state. These observations are in accordance with the conclusions of Fisher et al. (1995) based on the atomic structure of truncated *Dictyostelium* S1 in the presence of MgADP·BeF_x and MgADP·AlF_4^- and with results on the characteristics of the reactive SH_1 thiol (Phan et al., 1997), EPR spectroscopy (Ponomarev et al., 1995), and the shape of the cleft containing Trp510 (Park et al., 1996) in "trapped" Si−nucleotide complexes.

The effect of MgATP, MgADP, and $MgPP_i$ on the near-UV CD spectrum of myosin, HMM, and S1 was measured in the past by several investigators (Murphy, 1974; Cassim & Lin, 1975; Marsh et al., 1978; Chaussepied et al., 1986). These authors concur that both MgADP and MgATP perturb the near-UV CD spectrum of myosin and its active proteolytic fragments and the perturbations caused by the

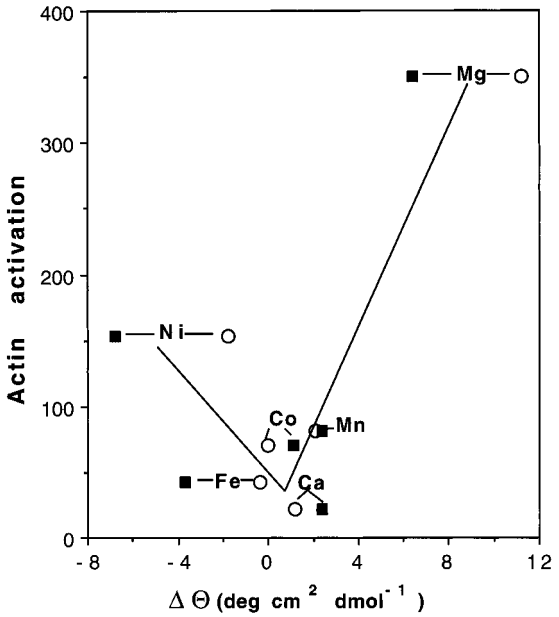

FIGURE 7: Correlation between actin activation of S1 ATPase versus ATP − ADP difference spectra of various metal divalent cations. Abscissa: molar ellipticity difference between S1 + MeATP and S1 + MeADP spectra at 259 (○) and 283 (■) nm. Ordinate: actin activation of S1 ATPase in the presence of metal ions expressed as V_{max} of actin-activated ATPase/ATPase in the absence of actin [see Table 1 of Peyser et al. (1996)].

nucleotides are different. However, there are discrepancies between the results presented by the various authors about the wavelength region and extent of the nucleotide- and $MgPP_i$-induced spectral changes. These discrepancies are probably due to different protein preparations (myosin, heavy meromyosin, S1) used in the various studies. Our results resemble most closely those of Chaussepied et al. (1986).

In this work, a number of divalent metal cations—Mg^{2+}, Mn^{2+}, Co^{2+}, Fe^{2+}, Ni^{2+}, and Ca^{2+} — have been studied with respect to their effect on the near-UV CD spectrum of S1 and S1 — nucleotide complexes. In the absence of nucleotides the cations (Mg^{2+}, Mn^{2+}, and Co^{2+}) did not or very slightly (Fe^{2+}, Ca^{2+}, and Ni^{2+}) affected the near-UV CD spectrum of S1, which indicates that the tertiary structure of S1 around the aromatic residues essentially remained unchanged upon addition of the metal ions. On the other hand, the nature of metal cations significantly affects the CD spectra obtained in the presence of nucleotides, which points the significant role of metal ions in the structure of the S1− nucleotide complexes. This is in accordance with our recent results on the effect of these metal ions on the actin activation of S1 ATPase and on the stability of the "trapped" S1·MeADP·PA complexes (Peyser et al., 1996). The effect of the nature of the metal ions on the vicinity of the aromatic residues is quite obvious when the spectra obtained in the presence of ADP and ATP are compared. In the presence of Mg^{2+} the difference between the ADP and ATP spectra are quite large especially in the region dominated by phenylalanine and tyrosine residues. This large change may reflect the essential conformational changes taking place during the dissociation of P_i, which is associated with the power stroke in the actomyosin motor system in the presence of the physiological Mg^{2+} ion. This can be best seen when plotting actin activation against $\Delta[\Theta]$ values of the ATP minus ADP difference spectra (Figure 7) in the presence of various metal ions. In the case of Mn^{2+}, Co^{2+}, and Ca^{2+}, the ADP and ATP spectra are essentially identical and, therefore, the $\Delta[\Theta]$ values are small, in correlation with the actin activation. In the presence of Fe^{2+}, the difference between the two spectra is mostly concentrated in the region of the ^1L_b transitions of tryptophans, the ADP values are being higher than those of ATP. This difference is even larger in the case of Ni^{2+}, the ADP spectrum being considerably blue shifted relative to the ATP spectrum. According to the generally accepted interpretation this may indicate that the solvent accessibility of the aromatic residues increases upon dissociation of P_i from the M**·NiADP·P_i transient state, when the M*·NiADP intermediate is formed (Woody, 1994). This unusual spectral effect may be due to the possible planar geometry assumed by Ni complexes, which is also reflected in a very low Ni-modulated ATPase activity in the absence of actin [see Table 1, Peyser et al. (1966)], and it correlates well with the higher actin activation value in the V-shaped plot (Figure 7). The S1·MeADP·BeF_x spectrum is also significantly influenced by the nature of the metal ions. In the presence of Mn^{2+} and Co^{2+} the BeF_x spectra are essentially identical to the ATP and ADP spectra, while with Mg^{2+}, Ca^{2+}, and Fe^{2+} they are different and run above the ADP spectra. As for the MeADP·AlF_4^- spectra in the presence of Co^{2+} and Ca^{2+} it is very close to spectra obtained with both the ADP and ATP, whereas with Mn^{2+} and Fe^{2+} large differences exist especially in Phe region where the ADP·AlF_4^- spectra run much below the other spectra.

We investigated the effect of the divalent cations on the fractional concentration distribution of steady-state myosin ATPase intermediates indicated in eq 1. Our estimation is based on the assumption that the S1·MeADP·BeF_x and S1·MeADP·AlF_4^- complexes closely mimic the M*·ATP and M**·ADP·P_i states, respectively. In the case of Mg^{2+} there is ample evidence which supports the above assumption. However, even with Mg^{2+} the results of Phan et al. (1997) indicate that the structures of the phosphate analog-containing complexes are similar but not identical with the intermediate states of the myosin-catalyzed ATP hydrolysis. In the case of non-native cations we only deduce that the analog-containing complexes mimic the intermediate states, but we do not have direct experimental evidence in this respect, which somewhat qualifies the validity of the distribution of the myosin ATPase intermediates in the presence of these cations.

It was shown previously that several of these cations increased the rate of ATP hydrolysis relative to that in the presence of Mg^{2+} and that the ATPase increase was correlated with the cation ionic radius (Peyser et al., 1996). Since P_i release is the rate limiting step in the presence of Mg^{2+}, these previous data suggested that the non-native divalent cations facilitate P_i release. Our current results indicate that the M*·ADP state is the predominant intermediate of the myosin ATPase in the presence of non-native divalent cations and therefore, the release of ADP is the rate-limiting step of this process. The results of Bagshaw (1975), which showed that the M**·ADP·P_i and M*·ADP states are about equally represented among the intermediates of S1 ATPase in the presence of Mn at 20 °C and M*·ADP becomes the predominant intermediate at 13 °C, support the above conclusion.

The non-native divalent cations also support the actin activated myosin ATPase (Peyser et al., 1996). According

to the above model in the presence of non-native cations the rate-limiting step is the ADP release, which suggests that in this case the actin activation of myosin ATPase is based on the acceleration of ADP release. This notion is supported by the finding that actin activates myosin ATPase in the presence of Mn^{2+} also at low temperature when M*·ADP is the predominant intermediate of the ATP hydrolysis (Hozumi & Tawada, 1975).

Force production during contraction results from the interaction of two proteins with spatial and time constraints imposed by the necessity that the binding site on myosin find its actin counterpart while myosin is appropriately configured to initiate energy transduction. The efficient coupling of ATPase to force production then dictates the selective enrichment of the myosin ATPase intermediate appropriate for actin binding and initiation of energy transduction, i.e., the M**·ADP·P_i state. When myosin and actin finally bind, actin acceleration of product release helps to ensure transduction and force production accompanies completion of the cycle. Our present findings, that the non-native divalent cations affect P_i release without actin, suggest that Mg^{2+} is responsible for populating the M**·ADP·P_i state in the absence of actin possibly by stabilizing the P_i in the active site. This possibility is consistent with the structure of ATP analogs in the active site of myosin where Mg^{2+} forms a bidentate chelate linking the β-phosphate and the γ-phosphate analog (Smith & Rayment, 1996).

In conclusion, we find that the near-UV CD spectrum distinguishes the various S1−nucleotide complexes that correspond to specific intermediates of the myosin-catalyzed ATP hydrolysis. The spectra of the "trapped" S1·MgADP·BeF_x and S1·MgADP·AlF_4^- complexes resemble to those of S1·MgATPγS and S1·MgADP·P_i, and, therefore, mimic the M*·ATP and M**·ADP·P_i transition states, respectively. In the presence of Mg^{2+} the ATP and ADP spectra are highly different, suggesting a large conformational change accompanying the M**·ADP·P_i → M*·ADP transition. Energy transduction in the molecular mechanism of muscle contraction can be viewed as a cyclical succession of transient S1 structures driven by ATP hydrolysis. Mg^{2+} plays a central role in stabilizing the key intermediate, the M**·ADP·P_i state, of the ATP hydrolysis, whose stability is an essential requirement of the power stroke. The nature of the metal cations present in the various S1−nucleotide complexes significantly affects the near-UV CD spectra and, therefore, the conformation of the complexes. The divalent cations have also a profound effect on the ATPase cycle by determining the rate-limiting step of the ATP hydrolysis. The use of divalent cations in place of Mg^{2+} is thus an elegant method for perturbing S1 structure to mimic intermediates in energy transduction.

ACKNOWLEDGMENT

The valuable technical assistance of Ms. Anda Rosen in the measurements of the CD spectra in Jerusalem is gratefully acknowledged.

REFERENCES

Ajtai, K., Peyser, Y. M., & Muhlrad, A. (1996) *Biophys. J. 70*, A161.

Applegate, D., & Reisler, E. (1984) *Biochemistry 23*, 4779−4784.

Bagshaw, C. R. (1975) *FEBS Lett. 58*, 197−201.

Bagshaw, C. R., & Trentham, D. R. (1974) *Biochem. J. 141*, 331−349.

Blotnick, E., & Muhlrad, A. (1994) *Biochemistry 33*, 6867−6876.

Cassim, J. Y., & Lin, T.-I. (1975) *J. Supramol. Struct. 3*, 510−519.

Chaussepied, P., Mornet, D., Barman, T. E., Travers, F., & Kassab, R. (1986) *Biochemistry 25*, 1141−1149.

Fisher, A. J., Smith, C. A., Thoden, J. B., Smith, R., Sutoh, K., Holden, H. M., & Rayment, I. (1995) *Biochemistry 34*, 8960−8972.

Fiske, C. H., & Subbarow, Y. (1925) *J. Biol. Chem. 66*, 375−400.

Goodno, C. C. (1979) *Proc. Natl. Acad. Sci. U.S.A. 76*, 2620−2624.

Grammer, J. C., Cremo, C. R., & Yount, R. G. (1988) *Biochemistry 27*, 8408−8415.

Hozumi, T., & Tawada, K. (1975) *Biochim. Biophys. Acta. 376*, 1−12.

Lymn, R. W., & Taylor, E. W. (1970) *Biochemistry 9*, 2975−2983.

Marsh, D., J. d'Albis, A., & Gratzer, W. (1978) *Eur. J. Biochem. 82*, 219−224.

Morita, F., & Yagi, K. (1966) *Biochem. Biophys. Res. Commun. 22*, 297−302.

Muhlrad, A., & Fabian, F. (1970) *Biochim. Biophys. Acta 216*, 422−427.

Muhlrad, A., & Hozumi, T. (1982) *Proc. Natl. Acad. Sci. U.S.A. 79*, 958−962.

Murphy, A. J. (1974) *Arch. Biochem. Biophys. 163*, 290−296.

Park, S., Ajtai, K., & Burghardt, T. P. (1996) *Biochim. Biophys. Acta 1296*, 1−4.

Peyser, Y. M., Ben-Hur, M., Werber, M. M., & Muhlrad, A. (1996) *Biochemistry 35*, 4409−4416.

Phan, B., & Reisler, E. (1992) *Biochemistry 31*, 4787−4793.

Phan, B. C., Cheung, P., & Reisler, E. (1995) *Biophys. J. 68*, A161.

Phan, B. C., Peyser, Y. M., Reisler, E., & Muhlrad, A. (1977) *Eur. J. Biochem. 243*, 636−642.

Ponomarev, M. A., Timofeev, V. P., & Levitsky, D. I. (1995) *FEBS Lett. 371*, 261−263.

Reisler, E., Burke, M., & Harrington, W. F. (1977) *Biochemistry 16*, 5187−5191.

Seidel, J. C. (1969) *Biophys. Biochim. Acta 189*, 162−170.

Setton, A., & Muhlrad, A. (1988) *J. Muscle Res. Cell Motility 9*, 132−146 (1988).

Smith, C. A., & Rayment, I. (1995) *Biochemistry 34*, 8973−8981.

Smith, C. A., & Rayment, I. (1996) *Biochemisty 35*, 5404−5417.

Strang, G. (1986) in *Introduction to Applied Mathematics*, pp 87−137, Wellesley-Cambridge Press, MA.

Strickland, E. H. (1974) *CRC Crit. Rev. Biochem. 2*, 113−175.

Tonomura, Y., Appel, P., & Morales, M. F. (1966) *Biochemistry 5*, 515−521.

Weeds, A. G., & Taylor, R. S. (1975) *Nature (London) 257*, 54−56.

Werber, M. M., Szent-Gyorgyi, A. G., & Fasman, G. (1972) *Biochemistry 11*, 2872−2883.

Werber, M. M., Szent-Gyorgyi, A. G., & Fasman, G. D. (1973) *J. Mechanochem. Cell Motility 2*, 35−43.

Werber, M. M., Peyser, Y. M., & Muhlrad, A. (1992) *Biochemistry 31*, 7190−7197.

Woody, R. W. (1994) in *Circular Dichroism: Principles and Application* (Nakanishi, K., Berova, N., & Woody, R. W., Eds.) pp 473−496, VCH Publishers, New York.

Yount, R. G., & Koshland, D. E. (1963) *J. Biol. Chem. 238*, 1708−1713.

BI970255Y